Published in Journal of Physics A: Mathematical and Theoretical , 2017, vol. 50 no. 7, which should be cited to refer to this work

Ultrasensitivity and sharp threshold theorems for multisite systems

M Dougoud[1], C Mazza[1] and L Vinckenbosch[1,2]

[1] University of Fribourg, Department of Mathematics, Chemin du Musée 23, CH-1700 Fribourg, Switzerland

[2] University of Applied Sciences and Arts Western Switzerland // HES-SO, HEIG-VD, Yverdon-les-Bains, Switzerland

E-mail: christian.mazza@unifr.ch

6 January 2017

Abstract. This work studies the ultrasensitivity of multisite binding processes where ligand molecules can bind to several binding sites. It considers more particularly recent models involving complex chemical reactions in allosteric phosphorylation processes and for transcription factors and nucleosomes competing for binding on DNA. New statistics-based formulas for the Hill coefficient and the effective Hill coefficient are provided and necessary conditions for a system to be ultrasensitive are exhibited. It is first shown that the ultrasensitivity of binding processes can be approached using sharp-threshold theorems which have been developed in applied probability theory and statistical mechanics for studying sharp threshold phenomena in reliability theory, random graph theory and percolation theory. Special classes of binding process are then introduced and are described as density dependent birth and death process. New precise large deviation results for the steady state distribution of the process are obtained, which permits to show that switch-like ultrasensitive responses are strongly related to the multi-modality of the steady state distribution. Ultrasensitivity occurs if and only if the entropy of the dynamical system has more than one global minimum for some critical ligand concentration. In this case, the Hill coefficient is proportional to the number of binding sites, and the systems is highly ultrasensitive. The classical effective Hill coefficient I is extended to a new cooperativity index I_q, for which we recommend the computation of a broad range of values of q instead of just the standard one $I = I_{0.9}$ corresponding to the 10% to 90% variation in the dose-response. It is shown that this single choice can sometimes mislead the conclusion by not detecting ultrasensitivity. This new approach allows a better understanding of multisite ultrasensitive systems and provides new tools for the design of such systems.

PACS numbers: XXX

Keywords: XXX, YYY, ZZZ

Submitted to: *J. Phys. A: Math. Theor.*

1. Introduction

Ultrasensitive responses, that is, switch-like input-output relationships are commonplace in signal transduction systems involving signaling cascades or bistable switches, see, e.g., the review articles [1, 2, 3, 4]. This work focuses on switching mechanisms based on multisite phosphorylation processes, and on multisite binding processes, where ligand molecules can bind to N binding sites. Such processes create thresholds such that the proportion of highly phosphorylated substrate is close to 0 when the ratio of kinase to phosphatase activity is below a critical level. The system is ultrasensitive if the response switches abruptly from a low to a high phosphorylation level when the ratio of kinase to phosphatase crosses this critical threshold. Usually this occurs when N is large, but having many phosphorylation sites is not sufficient to ensure ultrasensitivity, see [5, 6]. Various processes like protein or enzyme sequestration [7, 8] or allosteric mechanisms [9, 10, 8, 11, 12] are known to induce ultrasensitivity. It is therefore difficult to give a clear picture of all mechanisms leading to ultrasensitive responses.

Consider a macromolecule containing N sites $S = \{1, \cdots, N\}$ where ligand molecules can bind. The binary variables $n_i = 0,\ 1,\ i = 1, \cdots, N$ are used to describe site occupancy: $n_i = 1$ means that site i is occupied (or phosphorylated), while $n_i = 0$ indicates that no molecule is bound at site i. The *configuration space* is denoted by $\Lambda = \{n = (n_i)_{1 \le i \le N};\ n_i = 0,\ 1\}$, which has size $|\Lambda| = 2^N$. Let v denote the ligand concentration. The probability $\pi(n)$ to see a configuration n is assumed to be of the generic form

$$\pi(n) = \frac{\mu(n) v^{|n|}}{Z(v)}, \tag{1}$$

where the $\mu(n)$ are non-negative weights, $|n|$ denotes the number of bound sites, that is,

$$|n| = \sum_{i=1}^{N} n_i$$

and $Z(v)$ is the normalization constant $Z(v) = \sum_{n \in \Lambda} \mu(n) v^{|n|}$. In what follows, $\bar{\pi}$ denotes the law of $|n|$, which is defined on the set $\bar{\Lambda} = \{0, 1, \cdots, N\}$, and is such that

$$\bar{\pi}(k) = \sum_{n:\ |n|=k} \pi(n) = v^k \frac{\sum_{n:\ |n|=k} \mu(n)}{Z(v)}. \tag{2}$$

The mathematical expectation of any function $h(n)$ is denoted by $\mathbb{E}_\pi(h)$.

1.1. Transcription factors binding and transcription rates

In its simplest formulation, the expression of some gene is activated by the binding of transcription factors (TF) at a set of N binding sites. Let $v > 0$ denote the (TF) *concentration*. The *transcription rate*, that is the rate at which mRNAs are produced is often modeled using Hill functions of the form

$$f(v) = \frac{v^\eta}{K^\eta + v^\eta}, \tag{3}$$

where η is the so-called Hill exponent and K is the equilibrium constant of the chemical reaction. Switching systems are characterized by transcription rates that exhibit super steep behaviours in the neighbourhood of some critical concentration v_c, a typical example being a Hill function with a large coefficient η, see Fig. 1.

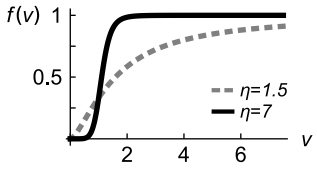

Figure 1: Hill functions for two Hill exponents $\eta = 1.5$ and $\eta = 7$. The larger η, the steeper the Hill function.

Hill functions are used as first order approximations, and more realistic models should encompass protein-protein interactions and cooperative effects, where the binding of a (TF) on DNA favours the binding of other molecules, see, e.g., [13]. Such interactions can be modeled using well-chosen probability measures π, see sections 1.2, 3 and 4. For arbitrary π, the related transcription rate can be modeled as the mean value of some increasing *activity function* a of the fractional ligation number

$$f(v) = \mathbb{E}_\pi(a(\frac{|n|}{N})). \tag{4}$$

It turns out that such responses can switch for well-chosen a even when sites are not interacting [14]. One recovers Hill functions when $a(x) \equiv x$, and when the probability π is so extreme that it puts positive weights only on the empty configuration $n = 0$ (that is $n_i \equiv 0$ for all i) and on the fully occupied configuration ($n_i \equiv 1$). In this particular all or none situation, binding sites act cooperatively, since they are either all vacant or all occupied.

Cooperativity is a well-known mechanism that can lead to steep and ultrasensitive responses, see [3]. Further in the text, we will introduce the Hill coefficient of cooperativity $\eta_H(v)$ for arbitrary binding probability π and for any ligand concentration $v > 0$, see section 2 . It is defined by comparing the mean fractional ligation number (4) to a Hill function (3). Classically, positive cooperativity holds when $\eta_H(v)$ is larger than one. This work focus on ultrasensitive multisite systems where the Hill exponent $\eta_H(v)$ is very large, and gives examples where it is asymptotically linear in N.

1.2. Modeling binding sites interactions using the Ising model

Interactions between binding sites or protein-protein interactions can be modeled by suitably choosing the probability π. A basic model which describes interactions between binding sites is the Boltzmann machine model (or Ising model). Consider the free energy function

$$H(n) = -\sum_{i \neq j} J_{ij} n_i n_j - \sum_i h_i n_i, \tag{5}$$

where the coefficients $J_{ij} = J_{ji}$ model pairwise interactions, and where the parameters h_i form a local field. One then defines the related Gibbs distribution

$$\pi_\beta(n) = \frac{1}{Z(\beta)} \exp(-\beta H(n)) v^{|n|},$$

where $\beta > 0$ is the inverse temperature. Such models appear in systems biology when modeling, e.g., transcription rates, see [15, 16] and the references therein. The model is said to be ferromagnetic when $J_{ij} \geq 0$. In this situation, assuming that $h_i \equiv 0$ and $v > 1$, the most probable configuration is the fully occupied one with $n_i \equiv 1$.

The mean field Curie-Weiss model corresponds to the case $J_{ij} \equiv J$, $i \neq j$, for some positive parameter J. In this case, the free energy function only depends on n through $|n|$, since $H(n) = -J|n|^2 + J|n|/2$, and therefore $\bar{\pi}(k) = v^k \binom{N}{k} \exp(\beta J(k^2 - k/2))/Z$, see (2).

Similar models have been studied in statistical mechanics, see [17, 18, 19, 20] and also within biological and biochemical frameworks, see [21, 22, 23], where links between switch like behaviours and phase transitions are established. The Ising model has been used, for example, to model transcription logic in prokaryotes [15], nucleosome positioning along the DNA [24], allosteric regulation [25, 26], or hysteresis in DNA compaction [23]. A well-known example is the case of regulation of the λ phage repressor where the O_R λ right operator contains three sites to which repressor dimers bind cooperatively. The authors of [27, 28] estimated the binding free energies to obtain empirically derived free energy functions H. It turns out that H corresponds to a free energy associated with a Boltzmann machine with up to three body interactions, which can be ferromagnetic and anti-ferromagnetic, see [16].

1.3. Competition for binding between nucleosomes and transcription factors

In eukaryotes, (TF) compete with multi-component complexes of histones and other proteins for DNA binding sites. Nucleosomes form the basic building blocks of chromatin, and are composed of histones around which DNA segments are wrapped. DNA accessibility to (TF) and RNA polymerase is then restricted by nucleosome and chromatin fiber. Transcription rates have been modeled using statistical-mechanical lattice models for protein-DNA binding and nucleosome arrangements along DNA, see [24, 29, 30, 31, 32, 33]. The model given in [34] shows how indirect cooperativity and ultrasensitivity can result from the competition between nucleosome positioning on the DNA and hampering (TF) trying to occupy free non-interacting binding sites on the DNA, see Fig. 2. Moreover, this mechanism, which has been well documented in vivo and in vitro, see [35, 36, 37, 38], is shown to be equivalent to the Monod-Wyman-Changeux allosteric model of cooperativity [39].

In the framework of this model, the state space is enlarged by considering pairs $(|n|, \text{off})$ and $(|n|, \text{on})$ where $|n|$ denotes the number of sites that are bound by (TF) and where the (on) and (off) variable indicates if the binding sites are accessible or not to (TF), see Fig. 2. The steady state is thus described by a probability on the set of

pairs (k, y), with $k \in \{0, 1, \cdots, N\}$ and $y \in \{\text{off}, \text{on}\}$. In this model, the binding sites are not interacting and identical, so that, the law of $|n|$ is binomial on each of the two on/off layers. The function of interest is then again of the form $f(v) = \mathbb{E}_{\bar{\pi}}(a(|n|/N))$, where $\bar{\pi}$ is the steady state marginal distribution of the first component. Such response curves are super steep in the neighbourhood of some critical concentration v_c. Similar statistical mechanical models have been developed to explain the allosteric Monod-Wyman-Changeux cooperativity [40]. Sections 5 and 6.1 propose a general and new way of understanding these phenomena using and developing new precise large deviations results for density dependent birth and death processes.

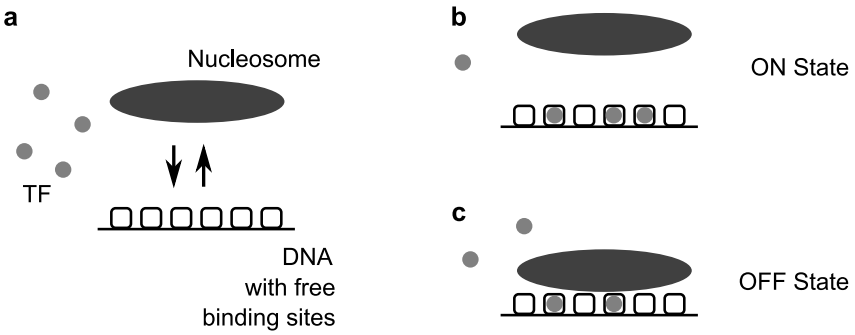

Figure 2: Nucleosome mediated cooperativity. (**a**) Transcription factors (TF) try to access free binding sites on the DNA. The nucleosome can bind/unbind only when all binding sites are free from (TF). (**b**) In the active (on) state, the nucleosome is unbound and (TF) can easily access the DNA. (**c**) In the inactive (off) state, the nucleosome is bound and hampers the access of (TF).

1.4. Phosphorylation processes

Phosphorylation and dephosphorylation processes play a fundamental role in eukaryotic signaling. Multisite phosphorylation with up to $N = 150$ sites in eukaryotes (see, e.g. [6]) form the basis for a strong switch-like response to an increase in kinase concentration. The authors of [41] have shown that such switches are strongly enhanced by non-essential phosphorylation sites. This mechanism is based on a model where a substrate molecule is active when the number of phosphorylated sites is larger than a threshold $\kappa_0 = \alpha N$, for some positive parameter $0 < \alpha < 1$. It turns out that phosphorylation processes can be ordered and unordered, see, e.g. [1]. In the first case, sites are being phosphorylated in a well defined order that is given by biochemistry, while in the unordered case, sites are being phosphorylated and dephosphorylated at random, see [16, 41].

Phosphorylation can be described using enzymatic reactions of the generic form

$$\mathrm{S}_k + \mathrm{E} \underset{\kappa_-^k}{\overset{\kappa_+^k}{\longleftrightarrow}} \mathrm{ES}_k \xrightarrow{\kappa_2^k} \mathrm{S}_{k+1} + \mathrm{E}, \tag{6}$$

(see, e.g, [41]), where S_k denotes a substrate molecule having k phosphorylated sites, and where E is the kinase. Similarly, dephosphorylation is represented by the reactions

$$S_{k+1} + F \underset{l_-^k}{\overset{l_+^k}{\leftrightarrow}} FS_{k+1} \xrightarrow{l_2^k} S_k + F, \tag{7}$$

where F is the phosphatase. These chemical reactions describe a Markov chain associated with the related chemical reaction networks. Forgetting the intermediate states composed of the complexes ES_k and FS_k, and just focusing on the states S_k, this Markov process is approximated by a birth and death process of steady state distribution $\bar{\pi}$. One can check that the steady state distribution associated with ordered phosphorylation is $\bar{\pi}(k) = v^k(v-1)/(v^{N+1}-1)$, where $v = \lambda u$ with u the ratio of the kinase to phosphatase concentrations and λ the relative phosphorylation efficiency. In the unordered case, the steady state is given by a binomial law of the form $\bar{\pi}(k) = \binom{N}{k} v^k/(1+v)^N$. The probability that a substrate molecule is active is then given by

$$f(v) = \pi(\frac{|n|}{N} \geq \alpha) = \bar{\pi}(\{\lceil \alpha N \rceil, \lceil \alpha N \rceil + 1, \cdots, N\}), \tag{8}$$

where $\lceil x \rceil$ denotes the ceiling function. This probability exhibits a super steep behaviour in the neighbourhood of a critical value v_c, see [16, 41].

1.5. Allosteric phosphorylation processes

The model proposed in [11] considers proteins that are either active (A) or inactive (I), and which have N sites that can be phosphorylated see Fig. 3. This is an adaptation of the classical Monod-Wyman-Changeux (MWC) model [39] which is one of the first model where ultrasensitivity was considered. Similar models have been studied using methods from statistical mechanics, see, e.g., [25, 26, 34, 40]. Interestingly, this model is used to study a newly discovered check point signalling pathway in budding yeast. The authors show that the known components of this pathway can form a robust hysteretic ultrasensitive switch, where a yeast bud first grows in a particular direction (polar growth) and next switches to isotropic growth.

Sections 5 and 6.2 give new techniques to handle such mechanisms using large deviation theory for birth and death processes. As for the model of section 1.3, the state space is enlarged by considering pairs (k, off) and (k, on), where k denotes the number of phosphorylated sites. The response function is again of the form $f(v) = \mathbb{E}_{\bar{\pi}}(a(|n|/N))$, where $\bar{\pi}$ is the steady state marginal distribution of the first component. In this model, the transition rate from (on) to (off) is strongly decreasing with the number of phosphorylated sites. This mechanism is responsible for the ultrasensitive behaviour, since it leads to the establishment of two stable equilibria corresponding to an (off) state for small k, and to an (on) state for large k.

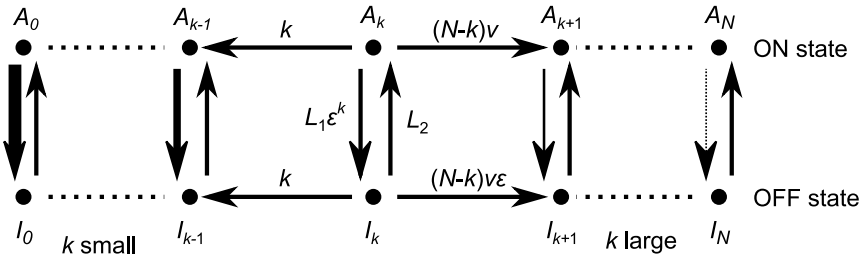

Figure 3: Allosteric phosphorylation. The process is a Markov Chain evolving along a strip. Arrows thickness illustrates that for small k, the transition toward (off) is strong, while for large k, it is weak.

1.6. Substrate-Catalyst reaction

Consider a substrate molecule containing N sites where ligand molecules can bind at rate v. The transition rates are provided in Fig. 4. This model has been used for example in [42] for proposing a mechanism depicting kinetic memory. The substrate-catalyst reactions

$$\mathrm{S}_k + \mathrm{C} \underset{L_2^k}{\overset{L_1^k}{\longleftrightarrow}} \mathrm{CS}_k \overset{k}{\longrightarrow} \mathrm{S}_{k-1}, \tag{9}$$

and the reactions associated with ligand binding

$$\mathrm{S}_k \overset{v(N-k)}{\longrightarrow} \mathrm{S}_{k+1}, \tag{10}$$

define a Markov chain evolving on a strip, see Fig. 4. The model described in section 1.4 considers analogous enzymatic reactions corresponding to (unordered) phosphorylation and dephosphorylation steps by forgetting intermediate complex species. It assumes also fast reactions and quasi-equilibrium in reactions (6) and (7), while the present model only assumes quasi-equilibrium for the phosphorylation step (10). The state space is here again described by pairs (k, S_k) and (k, CS_k). As in the previous model, the ratio between the transition rate towards (off) to the rate towards (on) decreases with k, as illustrated in Fig. 4. This results in a switch-like behaviour of the mean number of phosphorylated sites, since it leads two stable equilibria corresponding to an (off) state for small numbers of phosphorylated sites, and to an (on) state for a large number of phosphorylated sites, see sections 5 and 6.3 for further details.

1.7. Organization of the paper

The paper is organized as follows. Section 2 recalls the thermodynamical definitions of the Hill coefficient of cooperativity $\eta_H(v)$ and of the effective (or Goldbetter-Koshland) cooperativity index I, which are the two basic measures of cooperativity of common use in both empirical and theoretical studies in biochemistry, molecular biology and biophysics. Positive cooperativity in the Hill sense is next introduced for general response functions $f(v)$. Generalizations I_q of the effective Hill coefficient I are described

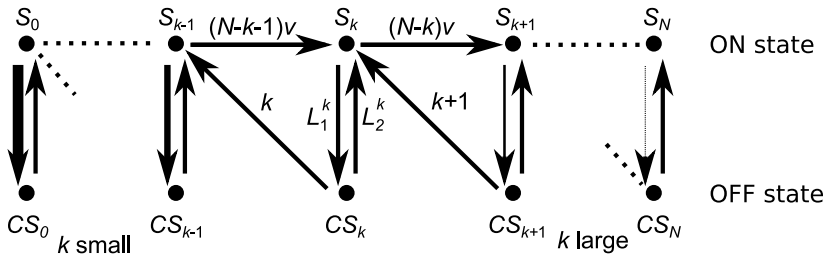

Figure 4: Transition scheme associated with substrate-catalyst reactions. L_1 and L_2 are such that $L_1 << L_2$ so that $(L_2/L_1)^k$ increases very fast, which is suggested by the arrows thickness showing that transitions towards (off) state are less and less likely as k becomes large.

following the results of [16]. Section 3 introduces the notion of site-specific Hill coefficient for binding processes. It allows to compare positive cooperativity in the Hill sense with local and microscopic positive cooperativity. Section 4 introduces the notion of influence function, which has been introduced to study sharp threshold phenomena in reliability theory, statistical mechanics and percolation theory, where functions exhibiting super sensitive behaviours are commonplace. Two fundamental inequalities giving lower bounds for the derivative of response functions are provided. This might be of interest for giving lower bound for finite size switch-like systems from systems biology. Section 5 develops new tools for studying a large class of models where ultrasensitive behaviours occur, including the models of sections 1.3, 1.5 and 1.6. These results are obtained using birth and death processes approximations and lead to the emergence of a global picture. We show that there exists a critical ligand concentration v_c for which $\eta_H(v_c)$ grows linearly in the number of binding sites if and only if some entropy function has more than one global minimizer. Section 6 revisits the examples given in sections 1.3, 1.5 and 1.6 using these new tools. Finally, details of computations, of formula derivation and proofs are provided in the Supplementary Information.

2. Measures of ultrasensitivity for general input-output responses

According to [2], ultrasensitivity is a property of steady states input-output response that makes them switch-like character. Goldbetter and Koshland [43, 44] defined a response function $f(v)$ to be ultrasensitive if it takes less than a 81-fold change in input concentration v to drive the output $f(v)$ from 10% to 90% of its maximum. This means that for increasing f, $v_{0.9} < 81\ v_{0.1}$, where the quantiles $v_{0.1}$ and $v_{0.9}$ are chosen so that $f(v_{0.1}) = 0.1\ f(\infty)$ and $f(v_{0.9}) = 0.9\ f(\infty)$. Hence, f is ultrasensitive when the so-called *Goldbetter-Koshland index* I is larger than one:

$$I = \frac{\ln(81)}{\ln(\frac{v_{0.9}}{v_{0.1}})} > 1. \tag{11}$$

The *Hill coefficient* $\eta_H(v)$ also provides a measure of steepness of dose-response functions. It is defined as

$$\eta_H(v) = \frac{\mathrm{d}}{\mathrm{d}\ln(v)} \ln\Big(\frac{f(v)}{f(\infty) - f(v)}\Big). \tag{12}$$

Basically, this coefficient is related to the derivative of f at v, and is thus large for steep curves. $\eta_H(v)$ can however be understood in various ways, using, e.g., affinity functions associated with generic chemical reactions, see [16, 45, 46].

Hill proposed $\eta_H(v)$ as an indicator of cooperativity by comparing f with Hill functions of the form (3) to get a Hill exponent η reflecting the degree of coooperativity of the system. Indeed, if f were proportional to a Hill function, one would have

$$\frac{f(v)}{f(\infty)} = \frac{v^\eta}{K^\eta + v^\eta}, \tag{13}$$

for positive K and η. In this case,

$$\ln\left(\frac{f(v)}{f(\infty) - f(v)}\right) = \eta\ln(v) - \eta\ln(K),$$

and $\eta_H(v)$ in (12) would simply be η, which explains the idea behind this definition. When for example f is the mean fractional ligation number of some multisite system, the following terminology is of current use:

- When $\eta_H(v) > 1$ for all $v > 0$, the system exhibits positive cooperativity in the Hill sense.
- When $\eta_H(v) < 1$ for all $v > 0$, one speaks o negative cooperativity in the Hill sense.
- The special case where $\eta_H(v) \equiv 1$ is synonomous with non-cooperativity.

The Golbetter-Koshland coefficient I and the Hill coefficient are closely related. To show this, let us introduce a more general definition of I that has already been given in [16]. When f is increasing, the ratio $0 \le f(v)/f(\infty) \le 1$ can be seen as a probability distribution function. Let $q \in [1/2, 1]$, and consider the quantiles v_q and v_{1-q} defined as $q = f(v_q)/f(\infty)$ and $1 - q = f(v_{1-q})/f(\infty)$. The *effective Hill coefficient* is defined by

$$I_q = \frac{2\ln(\frac{q}{1-q})}{\ln(\frac{v_q}{v_{1-q}})}. \tag{14}$$

The standard definition in (11) corresponds to the special choice $q = 0.9$, with $I = I_{0.9}$. Let $\bar\eta_H$ be such that $\eta_H(v) = \bar\eta_H(\ln(v))$. Then

$$I_q = \frac{1}{\ln(v_q) - \ln(v_{1-q})} \int_{\ln(v_{1-q})}^{\ln(v_q)} \bar\eta_H(y)\,\mathrm{d}y, \tag{15}$$

see [16] and [47].

In the following, we will focus on mechanisms leading to super sensitive or highly ultrasensitive responses where either I_q or $\eta_H(v)$ diverges to ∞ as $N \to \infty$ for some parameter q or for some critical concentration $v = v_c$.

3. Cooperativity and ultrasensitivity of binding processes

In the special case where the activity function is given by $a(x) \equiv x$, it will be useful in what follows to consider this nice formula for $\eta_H(v)$

$$\eta_H(v) = \frac{\mathrm{Var}_\pi(\frac{|n|}{N})}{\bar{p}(1-\bar{p})}\, N, \tag{16}$$

where $\bar{p} = \sum_i \pi(n_i = 1)/N$ and where Var_π denotes the variance under probability π, see [46, 48]. Indeed, one obtains that there is a critical concentration v_c such that $\eta_H(v_c) \sim CN$ as $N \to \infty$ for some positive constant C as $N \to \infty$ when $\mathrm{Var}_\pi(\frac{|n|}{N})/(\bar{p}(1-\bar{p})) \sim C$. The basic question is then to give conditions ensuring that the variance is asymptotically positive, see section 5.

There is an intuitive probabilistic picture behind positive cooperativity given by

$$\pi(\{\text{sites } i \text{ and } j \text{ are occupied}\}) \geq \pi(\{\text{site } i \text{ is occupied}\})\pi(\{\text{site } j \text{ is occupied}\}),$$

with a strict inequality for at least one pair of sites i and j, which suggests some synergistic effect, see [49]. Mathematically, this last inequality becomes

$$\mathrm{Cov}_\pi(n_i, n_j) \geq 0,$$

so that the random variables n_i and n_j are positively correlated when the above inequality is strict. A typical example where such inequalities hold is the ferro-magnetic Ising model, see section 1.2 or [20] for more details. This suggests to consider *site-specific Hill coefficients* $\eta_{H,i}(v)$ which measure the effect of the binding of a molecule at site i on the binding of molecules at sites different from i, see [45]. They are defined by [16]

$$\eta_{H,i}(v) = 1 + \mathbb{E}_\pi(\bar{n}_i | n_i = 1) - \mathbb{E}_\pi(\bar{n}_i | n_i = 0), \tag{17}$$

where $\mathbb{E}_\pi(\cdot | n_i = \cdot)$ denotes the conditional expectation under the probability measure π given the state of the site i, and where $\bar{n}_i = \sum_{j \neq i} n_j$ is the ligation number at sites different from i. The coefficient $\eta_{H,i}(v)$ gives thus the gain in bound molecules at site different from i when adding a molecule at site i, and should be larger than 1 for cooperative biochemical systems. One can check that

$$\eta_{H,i}(v) = 1 + \frac{\mathrm{Cov}_\pi(n_i, \bar{n}_i)}{\mathrm{Var}_\pi(n_i)} = 1 + \frac{\sum_{j \neq i} \mathrm{Cov}_\pi(n_i, n_j)}{p_i(1-p_i)}, \tag{18}$$

where $p_i = \pi(n_i = 1)$. Hence,

$$\mathrm{Cov}_\pi(n_i, \bar{n}_i) \geq 0 \quad \text{ if and only if } \quad \eta_{H,i} \geq 1. \tag{19}$$

Both kind of coefficients are related to each other by, see [16],

$$\eta_H(v) = \frac{\mathrm{Var}_\pi(|n|)}{N\bar{p}(1-\bar{p})} = \frac{\sum_i p_i(1-p_i)\eta_{H,i}(v)}{N\bar{p}(1-\bar{p})}. \tag{20}$$

Note that local positive cooperativity (19) at all sites i does not imply positive cooperativity in the Hill sense ($\eta_H > 1$). This is a consequence of (18) and (20), since $\sum_i p_i^2/N > (\sum p_i/N)^2$ for non-constant p_i. Hence, a system which exhibits negative cooperativity in the Hill sense ($\eta_H(v) < 1$) can be such that there is a site i with $\eta_{H,i}(v) > 1$ (see [46, 47] for discussions on this problematic). It is therefore necessary to consider the system in its entirety.

The following result provides a generalization of (16) for any activity function $a(x)$.

Theorem 1. *Let π be a probability measure of the form given in* (1) *and let $f(v)$ be given by* (4)*. Then,*

$$\eta_H(v) = \frac{\mathrm{Cov}_\pi(a(\frac{|n|}{N}), \frac{|n|}{N})a(\frac{k^*}{N})}{f(v)(a(\frac{k^*}{N}) - f(v))}\, N, \tag{21}$$

where k^* denotes the largest k for which there is a configuration n such that $|n| = k$ and $\mu(n) > 0$, in such a way that $a(\frac{k^*}{N}) = f(\infty)$. Moreover, $\lim_{v\to\infty} \eta_H(v) = \lim_{v\to 0} \eta_H(v) = 1$.

The proof can be found in the Supplementary Information.

4. Influence functions and sharp-thresholds

As seen previously, Hill coefficients $\eta_H(v)$ and their effective versions I_q are used to measure the steepness of binding curves in biological problems. Efficient genetic switches occur when the binding curve switches abruptly from a low saturation level to a high saturation level within a small concentration interval at the log scale. Similar switches occur in many frameworks of applied probability and statistical mechanics, like reliability theory, random graph theory and percolation theory, where sharp-threshold phenomena are commonplace. A well-developed theory to study such phenomena already exists [50, 51, 52, 53, 54]. In what follows, we will make links between these fields explicit. These results give general conditions ensuring the emergence of ultrasensitivity in systems biology.

4.1. Conditional influences

Let μ be a positive probability measure on the configuration space Λ, and define, for $0 < p < 1$, the new probability measure

$$\pi_p(n) = \frac{1}{Z_p}\mu(n)\prod_i \left(p^{n_i}(1-p)^{1-n_i}\right), \tag{22}$$

where Z_p is the normalization constant (or partition function). Then π_p coincides with a probability π given in (1) when the concentration v and p are such that $v = p/(1-p)$. Let $A \subset \Lambda$ be a subset of Λ. The *conditional influence* $I_A(i)$ is defined as

$$I_A(i) = \pi_p(A|n_i = 1) - \pi_p(A|n_i = 0), \tag{23}$$

that is,

$$I_A(i) = \mathbb{E}_{\pi_p}(\mathbf{1}_A | n_i = 1) - \mathbb{E}_{\pi_p}(\mathbf{1}_A | n_i = 0),$$

where $\mathbf{1}_A$ is the indicator function of the subset A. One sees that

$$\eta_{H,i}(v) = 1 + \sum_{j \neq i} I_{\{j\}}(i).$$

When π_p is a product measure with $p_i \equiv p$ and A is an *increasing event* (that is, if $n' \in A$ and $n' \leq n$, then $n \in A$), there exists an absolute positive constant c such that, for all N, $p \in]0,1[$, there exists $i \in \{1, \ldots, N\}$ such that

$$I_A(i) \geq c \min\{\pi_p(A), 1 - \pi_p(A)\} \frac{\ln(N)}{N}, \tag{24}$$

see [55, 56], where similar inequalities have been first studied for boolean functions, [51] where (24) was derived for more general functions using discrete Fourier and harmonic analysis, or [57] where such inequalities have been proven using probabilistic methods.

4.2. Conditional influence functions and sharp-thresholds

The aim of the sharp-threshold theory is to give conditions ensuring that the function $\pi_p(A)$ exhibits a sharp-threshold as p varies within a small interval of values of size $1/\ln(N)$. Such conditions are obtained using a Russo-type formula (see [52, 53]) of the form

$$\frac{\mathrm{d}\pi_p(A)}{\mathrm{d}p} = \frac{1}{p(1-p)} \operatorname{Cov}_{\pi_p}(\mathbf{1}_A, |n|), \tag{25}$$

which is similar to (21). We follow next [53] to introduce various probabilistic notions and a powerful theorem that yields results on sharp-thresholds. For $J \subset S$ and $\xi \in \Lambda$, let $\Lambda_J = \{0,1\}^J$ and

$$\Lambda_J^\xi = \{n \in \Lambda;\ n_j = \xi_j \text{ for } j \in S \setminus J\}.$$

The set of all subsets of Λ_J is denoted by $\mathcal{F}_J$. Let π be a positive probability measure on $(\Lambda, \mathcal{F}_S)$. The conditional probability measure π_J^ξ on $(\Lambda_J, \mathcal{F}_J)$ is defined by

$$\pi_J^\xi(n_J) = \pi(n_J | n_i = \xi_i \text{ for } i \in S \setminus J), \qquad n_J \in \Lambda_J.$$

The probability measure π is said to be *monotonic* when, for all $J \subset S$, all increasing subsets $A \subset \Lambda_J$, and all $\xi \in \Lambda$,

$$\pi_J^\xi(A) \leq \pi_J^\eta(A) \quad \text{ whenever } \xi \leq \eta. \tag{26}$$

It turns out that π is monotonic if and only if it is *1-monotonic*, that is, if (26) holds for all singleton sets J. The following result from [53] is very useful to obtain results on sharp-thresholds.

Theorem 2. *There exists a positive constant c such that the following holds. Let $A \in \mathcal{F}_S$ be an increasing event. Assume that π_p is monotonic for all p. If there exists a subgroup of the permutation group of N elements that acts transitively on S leaving both π and A invariant, then*

$$\frac{\mathrm{d}\pi_p(A)}{\mathrm{d}p} \geq \frac{c\alpha_p}{p(1-p)} \min\{\pi_p(A), 1-\pi_p(A)\} \ln(N), \tag{27}$$

where $\alpha_p = \pi_p(n_i)(1-\pi_p(n_i))$.

This implies that, for $0 < \varepsilon < 1/2$, the function $\tilde{f}(p) = \pi_p(A)$ increases from ε to $1-\varepsilon$ over an interval of values of p with length smaller in order than $1/\ln(N)$. This is precisely a sharp-threshold, which implies that the quantiles v_q and v_{1-q} with $q = 1-\varepsilon$ are such that $v_q - v_{1-q} \leq 1/\ln(N)$ leading to ultrasensitive behaviour.

5. Density dependent birth and death processes

This section considers probability distributions $\bar{\pi}_N$ on $\{0, 1, \cdots, N\}$ which are steady state distributions of density dependent birth and death processes. The derived results on ultrasensitivy will be then applied to the processes introduced in sections 1.3, 1.5 and 1.6. Let $c_k(t)$ denote the concentration of molecules with exactly k modified sites for phosphorylation processes, or, with exactly k bound ligand molecules for binding processes. The time evolution of these concentrations is often assumed to be of the form (see [10]),

$$\frac{\mathrm{d}c_k}{\mathrm{d}t} = b_{k-1}c_{k-1} - d_k c_k - b_k c_k + d_{k+1}c_{k+1}, \tag{28}$$

where b_k depends linearly on the inducer concentration v. In the above equation, it is assumed that c_k turns into c_{k+1} at the linear rate $b_k c_k$ and that c_{k+1} turns back into c_k at rate $d_{k+1}c_{k+1}$. This equation can be seen as the Kolmogorov forward equation associated with a birth and death process $Y_N(t)$ of birth rate $q_N(k, k+1) = b_k$ and death rate $q_N(k, k-1) = d_k$ (see e.g. [16]). This means that, for h small,

$$\mathbb{P}\left(Y_N(t+h) = k+1 \mid Y_N(t) = k\right) \sim b_k h$$

$$\mathbb{P}\left(Y_N(t+h) = k-1 \mid Y_N(t) = k\right) \sim d_k h.$$

Such processes are said to be *density dependent* when

$$q_N(k, k+1) = N b^{(N)}(\tfrac{k}{N}) \quad \text{and} \quad q_N(k, k-1) = N d^{(N)}(\tfrac{k}{N}),$$

for some functions $b^{(N)}$ and $d^{(N)}$. The birth rates $b^{(N)}$ and the death rates $d^{(N)}$ are given by Lipschitz-continuous functions on $[0,1]$, such that $b^{(N)} > 0$ and $d^{(N)} > 0$ on $]0,1[$, and $b^{(N)}(1) = d^{(N)}(0) = 0$. $b^{(N)}$ depends linearly on the inducer concentration v, so that the steady state distribution $\bar{\pi}_N$ has the form defined in (2). Assume for simplicity that

$$b^{(N)} - d^{(N)} \xrightarrow[N\to\infty]{} F \quad \text{and} \quad \ln\left(\frac{d^{(N)}}{b^{(N)}}\right) \xrightarrow[N\to\infty]{} \ln(r),$$

for some well-behaved functions F and r (see Supplementary Information Assumption 3 for further details). One can check that the rescaled process $X_N(t) = Y_N(t)/N$ converges as $N \to \infty$ towards the orbits of the ordinary differential equation (o.d.e.) (see [58])

$$\frac{\mathrm{d}x(t)}{\mathrm{d}t} = F(x(t)), \quad x(0) = x_0, \tag{29}$$

when $X_N(0) \longrightarrow x_0$, as $N \to \infty$. The free energy function J and the entropy function I are defined by

$$J(x) = \int_0^x \ln(r(u))\mathrm{d}u \quad \text{and} \quad I(x) = J(x) - J_0, \tag{30}$$

where $J_0 = \min_{x\in[0,1]} J(x)$. The author of [59] proved that the family of steady state distributions $\bar{\pi}_N$ satisfies a large deviation principle of rate function I. The steady state distribution of the process concentrates asymptotically in the neighbourhood of the global minima x_i of the entropy function I (see Lemma 12 in the Supplementary Information). We provide new precise large deviations estimates which are necessary to show that, under some assumptions, for any global minimizer x_i of I,

$$\lim_{N\to\infty} \bar{\pi}_N([x_i - \varepsilon, x_i + \varepsilon]) > 0, \tag{31}$$

for all $\varepsilon > 0$. On the other hand, classical large deviations results of [59] imply that $\bar{\pi}_N(A)$ converges exponentially fast towards 0 as $N \to \infty$ for any subset A which does not contain a global minimizer x_i of I.

5.1. The basic mechanism underlying ultrasensitiviy

The above precise large deviations results show that the limiting steady state charges asymptotically every neighbourhood of the global minimizers of the entropy function. We next explain in detail the fundamental mechanism that lies at the heart of the ultrasensitive behaviour for a large class of models. All of the previous results which have been obtained for this class of models were based on ad-hoc computations using various kind of approximations [60, 8, 11, 34, 42]. We propose here a new and global picture for this new class of ultrasensitive multisite systems.

Assume that there is a concentration v such that the limiting (o.d.e.) (29) has a finite number of stable equilibria $0 < x_1 < x_2 < \cdots < x_m < 1$ that minimize the entropy function I, with $I(x_i) = 0$, $i = 1, \ldots, m$. Equation (31) implies that the steady state $\bar{\pi}_N$ concentrates on the set of global minima.

Assuming for simplicity that $a(x) \equiv x$, the Hill coefficient associated with the steady state distribution $\bar{\pi}_N$ is given by formula (16) and it writes within the birth and death process context as

$$\eta_H(v) = \frac{\mathrm{Var}_{\bar{\pi}_N}(X_N)}{\mathbb{E}_{\bar{\pi}_N}(X_N)(1 - \mathbb{E}_{\bar{\pi}_N}(X_N))}\ N. \tag{32}$$

- *The unimodal case* $m = 1$. When there is a single miminizer $0 < x_1 < 1$, the variance $\sigma_N^2 = \mathrm{Var}_{\bar{\pi}_N}(X_N)$ converges towards 0, and the expected value $\mathbb{E}_{\bar{\pi}_N}(X_N)$ converges towards x_1, so that

$$\frac{\eta_H(v)}{N} \sim \frac{\sigma_N^2}{x_1(1-x_1)} \longrightarrow 0, \quad \text{as} \;\; N \to \infty,$$

  and the Hill coefficient is sublinear in N.

- *The multimodal case* $m \geq 2$. When the number of minimizers is larger that 1, the limiting variance σ^2 is positive and the expected value $\mathbb{E}_{\bar{\pi}_N}(X_N)$ converges towards a limiting positive constant $e_X > 0$. In this situation,

$$\frac{\eta_H(v)}{N} \sim \frac{\sigma^2}{e_X(1-e_X)} > 0,$$

  so that the system is ultrasensitive with a Hill coefficient of order N.

In all of the biological models provided in sections 1.3, 1.5 and 1.6, there is a critical concentration v_c such that the limiting (o.d.e.) has one global minimizer ($m = 1$) when $v \neq v_c$, and two global minimizers $0 < x_1 < x_2 < 1$ when $v = v_c$. This situation is illustrated in Fig. 5, where one can see that the steady state is unimodal when $v \neq v_c$ and bimodal when $v = v_c$. The Hill coefficient is of order N when $v = v_c$, and otherwise is sublinear in N. From (21), analogous results hold for more general increasing and continuous activity functions $a(x)$, see Theorem 4 of the Supplementary Information.

5.2. Sharp threshold and finite N inequalities

This section shows how the inequalities given in section 4 can be applied to finite size systems of interest in systems biology as those given in sections 1.3, 1.5 and 1.6. When the sites are identical, $\bar{\pi}_N(\frac{|n|}{N}) = \bar{\pi}(|n|) = \binom{N}{|n|}\pi(n)$ (see (2)) and the related probability measure is monotonic when

$$\frac{k+2}{N-k-1} d^{(N)}\,(k+1)\, b^{(N)}\,(k+1) \;>\; \frac{k+1}{N-k} d^{(N)}\,(k+2)\, b^{(N)}\,(k)\,, \tag{33}$$

for all $k = 0, .., N-2$. A typical increasing event of interest is $A_N = \{n;\ |n| > \alpha N\}$ for some threshold $\alpha > 0$, (see also section 1.4, where this kind of event has been used to model the effect of non-essential phosphorylation sites on ultrasensitivity). Section 5.1 explains the importance of bimodal steady states in ultrasensitive systems of this sort for large N. For finite N, (27) gives that

$$\frac{\mathrm{d}\pi(A_N)}{\mathrm{d}p} \geq \frac{c\alpha_p}{p(1-p)} \min\{\pi(A_N), 1-\pi(A_N)\} \ln(N)$$

where $\alpha_p = \pi(n_i)(1-\pi(n_i))$ and $p = \frac{v}{1+v}$ (or equivalently $v = \frac{p}{1-p}$). The steady states associated with the examples of sections 1.3, 1.5 and 1.6 all satisfy (33) (see sections 6.1, 6.2 and 6.3).

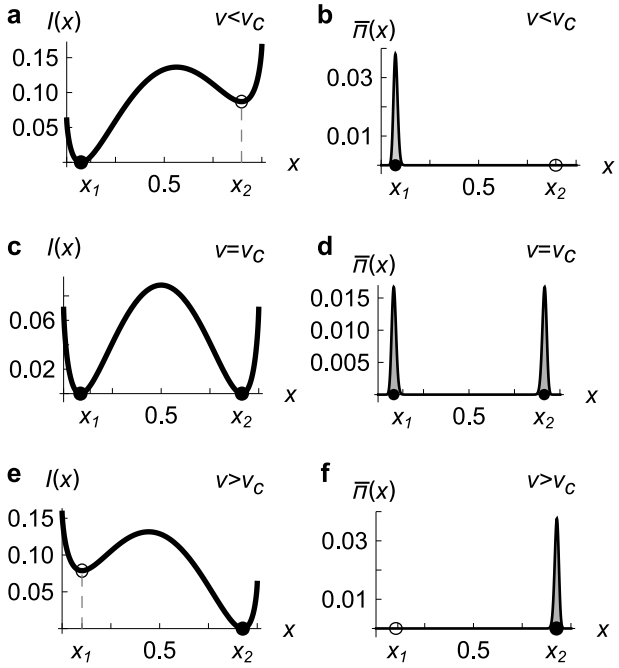

Figure 5: Bistability and steady state distribution for allosteric phosphorylation processes. The stable equilibria x_1 and x_2 of a bistable system are the local minima of the entropy function I. Bistable systems lead to bimodal steady state distributions and ultrasensitivity only when I possesses two global minima. (**a-b**) When $v < v_c$, the unique equilibrium x_1 minimizing $I(x)$ is the mode of the related unimodal steady state distribution $\bar{\pi}(x)$. (**c-d**) When $v = v_c$, both equilibria minimize I and the steady state distribution is bimodal of modes x_1 and x_2. In this case, the system exhibits ultrasensitivity with a Hill coefficient $\eta_H(v_c)$ linear in the number N of binding sites. (**e-f**) When $v > v_c$ the unique equilibrium minimizing I is $x_2 > x_1$ resulting in a unimodal steady state distribution.

Suppose that there is a single stable equilibrium x^* which minimizes the entropy function I, so that the Hill coefficient is sublinear in N, see section 5.1. The limiting steady state concentrates in any neighbourhood of x^*, and one can check that, when $\alpha = x^*$, $\liminf_N \pi(A_N) > 0$ and $\liminf_N \pi(A_N^c) > 0$, showing that the plot of this probability versus v or p becomes steep and exhibits a sharp threshold with a derivative lower bounded by $\ln(N)$. When $x^* \neq \alpha$, the inequality (27) is useless since large deviations estimates show that $\min\{\pi(A_N), 1 - \pi(A_N)\}$ converges exponentially fast toward 0 as $N \to \infty$.

6. Illustrations from systems biology

The results of section 5 apply to the models from systems biology which have been described in sections 1.3, 1.5 and 1.6. In these examples, the method follows three main steps:

(i) find the associated density-dependent birth and death process $Y_N(t)$ and the limiting (o.d.e.) (29);

(ii) compute the equilibria of this differential equation;

(iii) look for the global minimizer of the entropy function I as a function of v.

6.1. Nucleosome mediated cooperativity

This section studies the model introduced in section 1.3. Let us define a process $W(t)$ such that $W(t) = A$ if the nucleosome is not bound to the DNA at time t (active state) and $W(t) = I$ otherwise (inactive state). The DNA possesses N binding sites and the nucleosome can access or leave the DNA only when all binding sites are free of (TF). The transitions between active and inactive state occur at rate g (inactive to active) and κ (active to inactive), such that $L = g/\kappa = K^N$, see Fig. 6.

Let $N(t)$ denotes the number of occupied sites at time t. The birth rate is given by $\mu_A v$ in the active state and by $\mu_I v < \mu_A v$ in the inactive state. Here, v denotes the protein concentration. Fig. 6 sums up the whole process, which is equivalent to the Monod-Wyman-Changeux model of allosteric regulation [39] (see [12]).

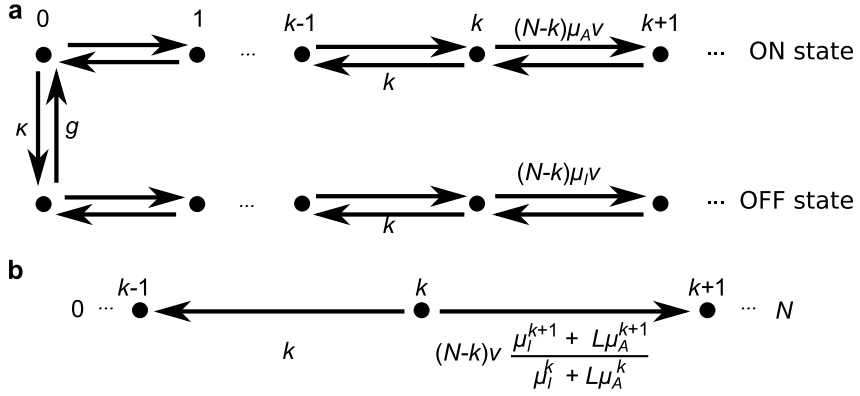

Figure 6: Nucleosome mediated cooperativity. (**a**) Description of the related birth and death process, which evolves on a three pieces component composed of two segments linked at their end. (**b**) The related birth and death process approximation $Y_N(t)$ as described in section 5.

Following [34] and [16] the full Markov-chain process $(N(t), W(t))$ at equilibrium is such that

$$\begin{aligned}\mathbb{P}\left(N(\infty) = k\,,\, W(\infty) = I\right) &= \frac{\binom{N}{k}\left(\mu_I v\right)^k}{\nu_I + L\nu_A},\\ \mathbb{P}\left(N(\infty) = k\,,\, W(\infty) = A\right) &= \frac{L\binom{N}{k}\left(\mu_A v\right)^k}{\nu_I + L\nu_A},\end{aligned}$$

where $\nu_I = \left(1 + \mu_I v\right)^N$ and $\nu_A = \left(1 + \mu_A v\right)^N$. This measure is the invariant measure of a birth and death process evolving in a three pieces component, see [16] and Fig. 6 (a).

A computation shows that

$$\mathbb{P}\left(W(\infty) = I \mid N(\infty) = k\right) = \frac{L\left(\mu_I v\right)^k}{L\left(\mu_I v\right)^k + \left(\mu_A v\right)^k},$$
$$\mathbb{P}\left(W(\infty) = A \mid N(\infty) = k\right) = \frac{\left(\mu_A v\right)^k}{L\left(\mu_I v\right)^k + \left(\mu_A v\right)^k}.$$

This leads to a birth and death process $Y_N(t)$ counting the number of bound sites in either the active or the inactive state, of birth and death rates $q_N\left(k, k+1\right)$ and $q_N\left(k, k-1\right)$, as in Fig 6 (b).

The associated limiting (o.d.e.) (29) is given by

$$\frac{\mathrm{d}x}{\mathrm{d}t} = \begin{cases} (1-x)\mu_A v - x, & \text{for } x > x_c, \\ (1-x)\mu_I v - x, & \text{for } x < x_c, \end{cases} \tag{34}$$

where $x_c = \frac{\ln(1/K)}{\ln(\mu_A/\mu_I)}$. It possesses two stable equilibria $x_1 = \frac{v\mu_I}{1+v\mu_I}$ and $x_2 = \frac{v\mu_A}{1+v\mu_A}$ which are functions of v. They both belong to $[0,1]$ when $1 > K > \frac{\mu_I}{\mu_A}$. A direct computation shows that both equilibria x_1 and x_2 are global minima of the entropy $I(x)$ when v is equal to the critical concentration $v = v_c = \frac{1-K}{K\mu_A - \mu_I}$. The limiting stationary distribution of the birth and death process converges to a probability measure $\bar{\pi}$ which is a mixture of Dirac measures concentrated at the equilibria x_1 and x_2. Fig. 7 provides two illustrations corresponding to the cases where $v \neq v_c$ and $v = v_c$, the latter situation leading to a bimodal steady state with a Hill coefficient $\eta_H(v_c)$ which is linear in the number of binding sites N. The explicit form of $\bar{\pi}_N$ and $I(x)$ are given in equations (10) and (13) of the Supplementary Information. In Fig. 8, one sees that the effective Hill coefficient I_q detects the switch-like response for an appropriate choice of q.

6.2. Allosteric phosphorylation processes

This section applies the results presented previously to the biological model introduced in section 1.5. For this model, in settings that will be made precise, it is possible to find explicit formulas and apply Theorem 1, as well as the birth and death process approach described in section 5 in order to study the sensitivity of the system. The reader is referred to section 3.2 of the Supplementary Information for further details, and more particularly to Propositions 5 and 6.

We follow [10, 11, 14] using a probabilistic framework. Let $W(t)$ be the Markov chain associated with the protein activity ($W(t) \in \{I, A\}$). The number of phosphorylated sites at time t is described by a process $N(t)$, so that the full process is given by a bivariate time-continuous Markov chain $(N(t), W(t))$. The authors of [10, 11, 14] opt for Markov chains of the transition rates that are given in Fig. 3, with $\varepsilon < 1$ small. See also [9] where the reason for taking ε^k in the switching rates is motivated using free energies.

Following [11, 14], suppose that $L_1 = L_1(N) = \varepsilon^{-N/2}$ and $L_2 \equiv 1$. In this settings, the steady state distribution of $N(t)$ is a mixture of two binomial distributions

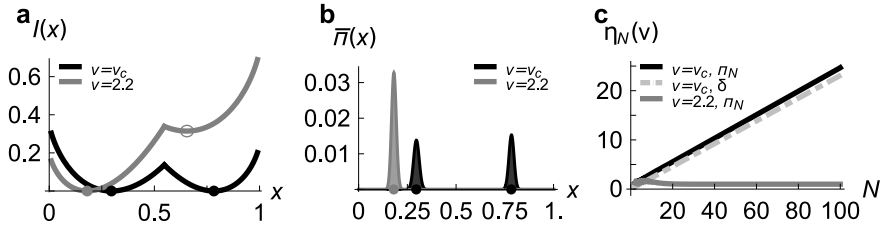

Figure 7: Bistability and ultrasensitivity in nucleosome mediated cooperativity. The parameters are set to $\mu_I = 0.1$, $\mu_A = 0.86$ and $K = 0.3$ which satisfy the conditions ensuring the existence of two minimizers. (**a**) The entropy function $I(x)$ possesses two roots when $v = v_c$ and only one when $v \neq v_c$. (**b**) The stationary distribution $\bar{\pi}_N$ is bimodal when $v = v_c$ (illustrated for $N = 1000$) and unimodal when $v \neq v_c$. The modes are situated at x_1 and (or) x_2, the zeros of $I(x)$. (**c**) The Hill coefficient $\eta_N(v)$ has been numerically computed with formula (21) with the distribution $\bar{\pi}_N$ ($v = v_c$ in black and $v \neq v_c$ in continuous grey line). It is proportional to N when $v = v_c$ and the system is ultrasensitive. It is also compared with the coefficient obtained with the limiting distribution when $v = v_c$, that is a mixture of Dirac masses (dotted line).

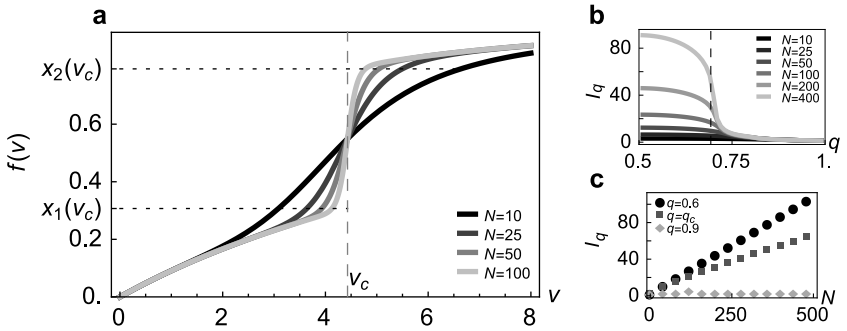

Figure 8: Numerical approximation of the effective Hill coefficient I_q in nucleosome mediated cooperativity. The parameters are set to $\mu_I = 0.1$, $\mu_A = 0.86$ and $K = 0.3$ and $a(x) \equiv x$. (**a**) Activity of the macromolecule $f(v) = \mathbb{E}_{\bar{\pi}_N}(a(\frac{|n|}{N}))$ for different values of N. When $q < \min\{x_2(v_c),\, 1 - x_1(v_c)\}$, I_q goes to infinity when $N \to \infty$. Otherwise I_q converges towards a constant. (**b**) I_q as a function of q for several values of N. (**c**) I_q as a function of N for three values of q.

$\mathcal{B}(N, \frac{\varepsilon v}{1+\varepsilon v})$ and $\mathcal{B}(N, \frac{v}{1+v})$, which, once rescaled on $[0, 1]$, concentrate respectively on $x_1 = \varepsilon v/(1 + \varepsilon v)$ and $x_2 = v/(1 + v)$ as the number of sites grows. The limiting behaviour of this mixture depends on the value of the concentration v with respect to the critical value $v_c = 1/\sqrt{\varepsilon}$: (i) if $v < v_c$, then the steady state distribution converges to a Dirac measure on x_1; (ii) if $v > v_c$, then it converges to a Dirac measure on x_2; (iii) if $v = v_c$, then it converges to a mixture of two half Dirac measures on x_1 and x_2 respectively.

Assuming now that the activity function a is continuous, bounded and strictly increasing on the unit interval, this particular form of $\bar{\pi}$ allows to compute explicitly

the Hill coefficient in the limit when $N \to \infty$ using the thermodynamical formula (21). We end up with two cases:

- when $v \neq v_c$, $\eta_H(v)$ is asymptotically constant;
- when $v = v_c$, $\eta_H(v_c)$ is asymptotically linear in N

$$\eta_H(v_c) \sim C_{v_c} N, \tag{35}$$

for some positive constant $C_{v_c} > 0$, so that the system is highly ultrasensitive.

This latter case is illustrated in Fig. 9.

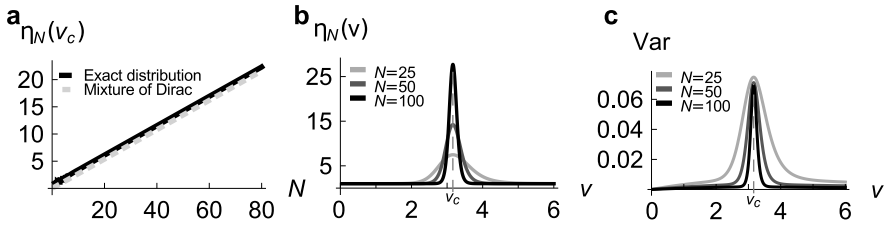

Figure 9: Hill coefficient for allosteric phosphorylation processes for $\varepsilon = 0.1$ and $a(x) = \frac{x}{1+x}$. (**a**) Hill coefficient with respect to N when $v = v_c$: explicit value (continuous line) and simulated value (dotted line) obtained by equation (21) with a mixture of Dirac random variables $\pi = \frac{1}{2}\delta_{x_1} + \frac{1}{2}\delta_{x_2}$. (**b-c**) $\eta_H(v)$ and $\mathrm{Var}_{\bar{\pi}_N}(X_N)$ as functions of v, for different values of N. They concentrate on their maximum at $v = v_c$ as N grows.

On the other hand, using the birth and death process approach described in section 5, the same steady state distribution appears and the stable equilibria of the limiting (o.d.e) (29) coincide with x_1 and x_2 so that, we get back to same conclusion as above. Consider the processes obtained by assuming fast switching rates between the active and inactive states, see e.g. [16, p.46]. Given that $N(t) = k$, the fast process $W(t)$ evolves according to the quasi-equilibrium

$$\mathbb{P}\left(W(\infty) = I \mid N(\infty) = k\right) = \sigma_k(I) = \frac{\varepsilon^{-\frac{1}{2}(N-2k)}}{1 + \varepsilon^{-\frac{1}{2}(N-2k)}}$$
$$\mathbb{P}\left(W(\infty) = A \mid N(\infty) = k\right) = \sigma_k(A) = \frac{1}{1 + \varepsilon^{-\frac{1}{2}(N-2k)}}.$$

The pair process $(N(t), W(t))$ is then replaced by a birth and death process $Y_N(t)$ whose birth and death rates $q_N(k, k+1)$ and $q_N(k, k-1)$ are given in Fig. 10 and whose steady state measure $\bar{\pi}_N$ coincides with the mixture $\bar{\pi}$ above. The associated limiting (o.d.e.) (29) is

$$\frac{\mathrm{d}x}{\mathrm{d}t} = \begin{cases} (1-x)\varepsilon v - x, & \text{if } 0 \leq x < 1/2, \\ (1-x)v - x, & \text{if } 1/2 \leq x \leq 1, \end{cases} \tag{36}$$

which possesses two stable equilibria x_1 and x_2. These are minimizers of the entropy I and are both are global minima if and only if $v = v_c = 1/\sqrt{\varepsilon}$, as illustrated in Fig. 11.

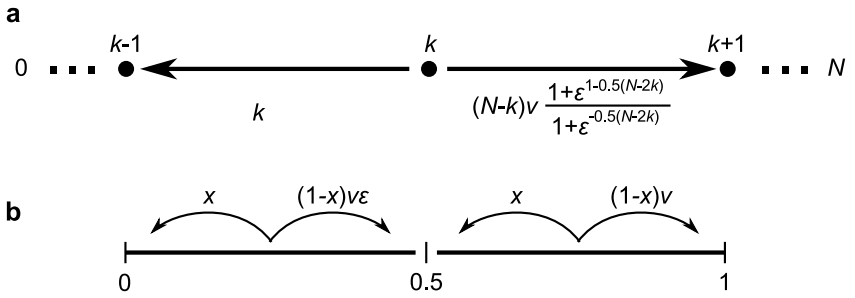

Figure 10: Schematic representation of the approximate allosteric phosphorylation process. (**a**) Quasi-equilibrium approximation. (**b**) Density dependent birth and death process approximation when $N \to \infty$.

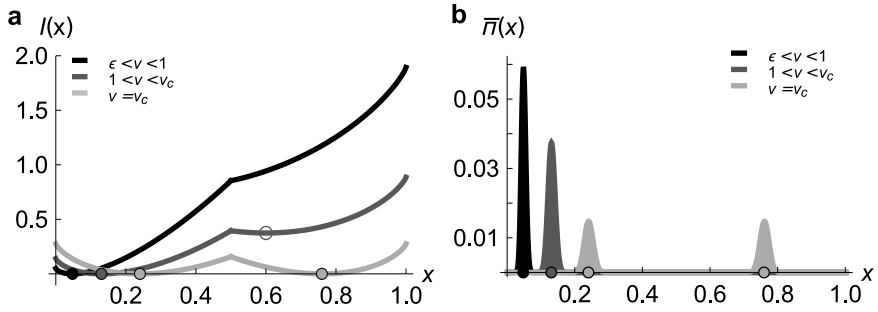

Figure 11: Steady state distribution of a phosphorylation process is unimodal when $v \neq v_c$ and bimodal when $v = v_c$. (**a**) The entropy function $I(x) = J(x) - J_0$ for different values of v and for $\varepsilon = 0.1$ (See section 3.2.4. in the Supplementary Information). The minima are highlighted with dots. When $v = v_c = 1/\sqrt{\varepsilon}$, $I(x)$ possesses two global minima. (**b**) The measure $\bar{\pi}_N$ concentrates at the global minima (plain dots) of the entropy function. This is illustrated for $N = 1000$.

Therefore, the case $v = v_c$ leads to a bimodal steady state in the limit and the Hill coefficient is of order N (ultrasensitive system), as described in section 5.1.

Finally, in the particular case when $a(x) \equiv x$, it is possible to compute explicitly $f(v)$ (see Supplementary Information). As one can see in Fig. 12 (a), larger N produce steeper curves, with a switch occurring around $v = v_c$, in accordance with our findings concerning $\eta_H(v_c)$. Consider the quantile $v_q^{(N)}$ given by the equation $q = f(v_q^{(N)})$. Lemma 7 of the Supplementary Information shows that for $a(x) = x$ and $1/2 \leq q \leq 1/(1+\sqrt{\varepsilon})$, one has $\lim_{N\to\infty} v_q^{(N)} = \lim_{N\to\infty} v_{1-q}^{(N)} = v_c$, so that

$$\lim_{N\to\infty} I_q = +\infty.$$

Fig. 12 (b) and (c) show that I_q is asymptotically linear in N. However, if q is close to 1, then I_q is asymptotically constant, so that one does not detect ultrasensitivity of order N. This shows the importance of using a broad range of coefficients I_q instead of only looking at the classical index $I_{q=0.9}$.

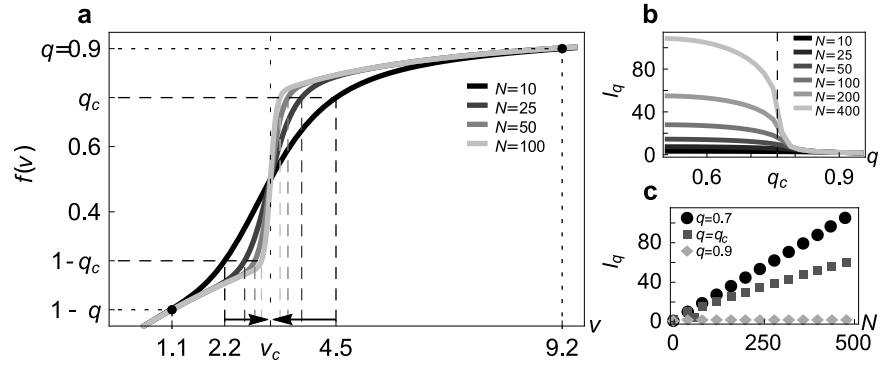

Figure 12: Numerical approximation of the effective Hill coefficient, equation (14), in the framework of allosteric phosphorylation processes. The activity function is $a(x) = x$ and $\varepsilon = 0.1$, such that $v_c = \sqrt{\varepsilon}^{-1} \approx 3.2$ and $x_2 \approx 0.76$. (**a**) The activity of the macromolecule $f(v)$ for different values of N. When $q = 0.9$, $v_{0.9}$ and $v_{0.1}$ converge to different limits when N grows. When q is smaller than the threshold $q_c = x_2(v_c)$, $v_q^{(N)} - v_{1-q}^{(N)}$ converges towards zero so that I_q goes to infinity. (**b**) The effective Hill coefficient I_q as a function of q for several values of N and (**c**), as a function of N, for three values of q. The index I_q, in broad outline, takes two values. The first one goes to infinity with N and the second one goes to 1, for larger q.

In conclusion, we see that the effective Hill coefficient I_q, which is nothing but an average of Hill coefficients (see (15)), diverges as $N \to \infty$ for a broad range of values of q, whereas the Hill coefficient $\eta_H(v_c) \sim C_{v_c} N$ only when $v = v_c$. Detection of ultrasensitivity should therefore be easier with I_q than with $\eta_H(v)$.

6.3. Substrate-Catalyst reactions

This section considers the model given in section 1.6. The catalytic reactions are simplified by assuming fast formation of the complex CS_k. To this extent, let be L_1^k, $L_2^k \gg 1$ for every $0 \leq k \leq N$. This last assumption leads to an approximating birth and death process $Y_N(t)$, of transition rates $q_N(k, k+1)$ and $q_N(k, k-1)$ given in Fig. 13. Following [42], set

$$L_k = \frac{L_2^k}{L_1^k} = \frac{L_2^0}{L_1^0}\gamma^{\frac{k}{N}} = L_0\gamma^{\frac{k}{N}}$$

for some positive constant γ. The related limiting (o.d.e.) is

$$\frac{\mathrm{d}x}{\mathrm{d}t} = \frac{v(1-x)L_0\gamma^x - x}{L_0\gamma^x + 1}, \tag{37}$$

and may possess multiple stable equilibria depending on the value of γ, v and L_0. Conditions leading to ultra sensitivity are detailed in section 3 of Supplementary Information. This happens, as for the previous examples and as illustrated in Fig. 14, for a critical concentration $v = v_c$. In this case, the entropy of the system possesses

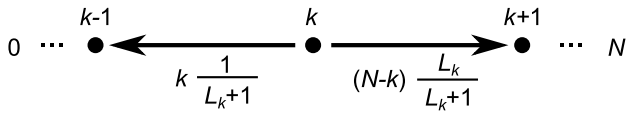

Figure 13: Transition rates associated with the birth and death process approximation of the substrate-catalyst reactions model.

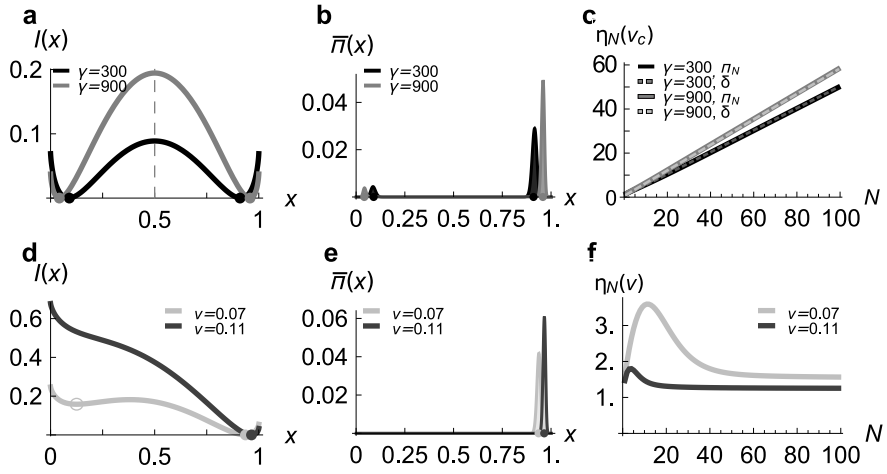

Figure 14: Bistability, bimodal distribution and ultrasensitivity for the substrate-catalyst reactions model. Here, $a(x) = x$. (**a-b-c**) Comparison with two values of γ when the concentration is critical $v = v_c$. (**d-e-f**) Comparison with two values of $v \neq v_c$ with $\gamma = 300$. (**a**) The entropy $I(x)$ has two global minima and a local maximum, the unstable equilibrium of (37) . (**b**) The steady state $\bar{\pi}_N$ converges towards a mixture of two Dirac masses. Here, $N = 1000$. (**c**) The Hill coefficient (32) computed with $\bar{\pi}_N$ is of order N (continuous lines) and follows the same trend as if computed with the limiting stationary distribution (dotted lines). (**d**) When $v \neq v_c$, $I(x)$ has two minima, but only one of them (plain disks) is global. (**e**) The stationary distribution is unimodal. Here, $N = 1000$. (**f**) The system does not exhibit ultrasensitivity.

two global minima, the steady state is bimodal and consequently the Hill coefficient is proportional to N, see Fig. 14 (a-c). Otherwise, the Hill coefficient is asymptotically constant, see Fig. 14 (d-f). Fig. 15 shows that to detect ultra-sensitivity with the effective Hill coefficient I_q, q has to be smaller than x_2, the second stable equilibrium of (37), when $v = v_c$. Various plots of f for increasing values of N are represented with the global finding that the effective Hill coefficient I_q is proportional to N for sufficiently small q.

7. Conclusion

Multisite binding systems or phosphorylation processes are essential features of many switch-like responses in signal transduction. Various mechanisms are known to generate

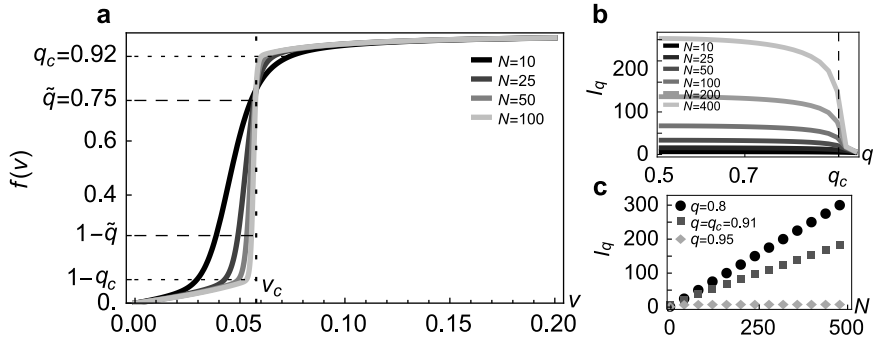

Figure 15: Numerical approximation of the effective Hill coefficient, equation (14), for the substrate-catalyst reactions model. Here, $a(x) = x$, $\gamma = 300$ and $L_0 = 1$. In this case $v_c \approx 0.057$ and $x_2 \approx 0.92$. (**a**) The activity of the macromolecule $f(v) = \mathbb{E}_{\bar{\pi}_N}(\frac{|n|}{N})$ for different values of N. Ultrasensitivity is detected for the standard $q = 0.9$ since $0.9 < x_2(v_c) = q_c$ and I_q goes to infinity. (**b**) Plot of the effective Hill coefficient versus q for several values of N, and (**c**), as a function of N, for three values of q. The related measure $\bar{\pi}_N$ is given in equation (20) of the Supplementary Information

.

ultrasensitive behaviours where a small change in ligand concentration leads to an abrupt change of the response function output. Cooperativity and synergistic effects where modifications at some site directly or indirectly increase the rate of modification of neighbouring sites are particularly well known mechanisms that lead to switch-like outputs. This work models binding sites and protein-protein interactions, or enzymatic phosphorylation chemical reactions using probability measures π that are defined on the configuration space composed of the possible states $n = (n_i)$ of the system, and that depend on the ligand concentration $v > 0$. A recent work of [14] has shown that response functions that are the statistical averages of non-linear functions $a(|n|/N)$ of the fractional ligation number can switch even when binding sites are not interacting. This occurs for example when considering non-essential phosphorylation sites where a is a threshold like function which vanishes when the number of phosphorylated sites is smaller that a fraction κN of the total number N of binding sites, and is set to 1 otherwise. In most studied multisite systems, the activation function a is however linear. In this case, binding sites interactions and positive cooperativity play a major role for producing switch-like responses functions. A different class of examples from systems biology is provided in sections 1.3, 1.5 and 1.6, which model allosteric regulation. In these examples, binding sites are not interacting, and the activity function is linear. This work gives new tools for understanding and studying ultrasensitivity within these various classes of models.

Section 1.2 introduces the Ising model which is one of the most typical example of statistical mechanical lattice model of interacting binding sites; in this setting, local positive cooperativity is modelled by choosing ferro-magnetic coupling constants. For example, mean field Curie-Weiss models have been used in biological frameworks to

consider long-range interactions, and the switch-like behaviour of the mean fractional ligation number has been associated to phase transitions [17, 19, 20, 21].

The models given in sections 1.3, 1.5 and 1.6 introduce three examples of biochemical processes which are given through transition rates that define Markov chains. The first model is concerned with the competition for binding on DNA between nucleosomes and transcription factors, while the second one deals with phosphorylation processes that control the activity of proteins. Both dynamics can be seen as allosteric regulation processes, where the binding of ligand molecules can alter enzymatic and protein activity via allosteric communication. Recent research, see, e.g., [61, 62, 63], led to the discovery of hidden allosteric pockets that control the activity of proteins, but that are not present in conventional crystallographic structures. Pharmaceutics exploits such hidden allosteric sites by designing drug-like molecules that bind to such pockets to control protein activity. The methods developed in this paper might thus be useful for the design of such therapeutic molecules.

Sections 2 and 3 introduce basic measures of cooperativity like the Hill coefficient $\eta_H(v)$, site-specific Hill coefficients and a new effective Hill coefficient I_q, for which we recommend the computation of a broad range of values of q instead of just the standard one $I = I_{0.9}$ corresponding to the 10% to 90% variation in the dose-response. It is shown that this single choice can sometimes mislead the conclusion by not detecting sharp thresholds. The paper focus on ultrasensitivity where there is a critical ligand concentration $v = v_c$ such that $\eta_H(v_c)$ is asymptotically linear in the number of binding sites N, by recalling results from statistical mechanics on sharp threshold phenomena, and by proposing a completely new approach based on large deviations for birth and death processes.

Section 4 recalls results from probability theory and statistical mechanics where systems exhibiting sharp thresholds are commonplace. Theorem 2 gives a useful inequality that can be used to check if the steady state distribution of a given finite size stochastic process leads to super steep responses.

When such dynamical processes can be approximated by density dependent birth and death processes, new mathematical results on precise large deviations for the related steady state distributions are obtained. A new and global picture emerges in section 5.1: it is shown that the asymptotic behaviour of the Hill coefficient is strongly related to the existence of multiple stable equilibria of a related (o.d.e.). The existence of a critical ligand concentration v_c such that $\eta_H(v_c)$ is asymptotically linear in N is strongly related to the existence of at least two stable equilibria of the (o.d.e.) that are global minimizers of the entropy function of the dynamical system.

This occurs in the examples of sections 1.3, 1.5 and 1.6. In these models, the transition diagrams define Markov chains that are evolving on planar strips where the nodes are given by pairs (k, off) and (k, on), where k denotes the number of bound (TF) or the number of phosphorylated sites, and the second component gives the activity level of the protein. In this framework, the binding probability is given by the marginal steady state distribution associated to the first component k. The transition rates are

designed to favour the (off) state for small k and the (on) state for large values of k. As a consequence of this mechanism, the limiting (o.d.e.) has one stable equilibrium x_1 which is associated with small values of k and to the (off) state, and one another stable equilibrium $x_2 > x_1$ corresponding to large values of k and to the (on) state. When the ligand concentration is such that $v < v_c$, the entropy function is minimized for $x = x_1$ and the related steady state is unimodal of mode x_1, so that the Hill coefficient is sublinear in N. When $v > v_c$, a similar picture holds for $x = x_2$. When $v = v_c$, both stable equilibria minimize the entropy. In this case, the steady state is bimodal and the Hill coefficient $\eta_H(v_c)$ is asymptotically linear in the number of binding sites. This new approach allows a better understanding of multisite ultrasensitive systems and provides new tools for the design of such systems.

Acknowledgments

We are grateful to our colleague Ioan Manolescu for helpful discussions on sharp-threshold results and influence functions. We are also grateful to the referees for their helpful comments on an earlier version of the manuscript.

References

[1] Salazar C and Höfer T 2009 *FEBS Journal* **276** 3177–3198
[2] Ferrell J E and Ha S H 2014 *Trends in Biochemical Sciences* **39** 496–503
[3] Ferrell J E and Ha S H 2014 *Trends in Biochemical Sciences* **39** 556–569
[4] Ferrell J E and Ha S H 2014 *Trends in Biochemical Sciences* **39** 612–618
[5] Gunawardena J 2005 *Proceedings of the National Academy of Sciences* **102** 14617–14622
[6] Thomson M and Gunawardena J 2009 *Nature* **460** 274–277
[7] Buchler N E and Cross F R 2009 *Molecular Systems Biology* **5:272**
[8] Martins B M C and Swain P S 2013 *PLoS Computational Biology* **9** e1003175
[9] van Zon J S, Lubensky D K, Altena R H and ten Wolde P R 2007 *Proceedings of the National Academy of Sciences* **104** 7420–7425
[10] Enciso G A 2013 *Lecture Notes in Mathematics* **2102** 199–224
[11] Enciso G, Kellogg D R and Vargas A 2014 *PLoS Computational Biology* **10** e1003443
[12] Edelstein S J 2014 *Journal of Molecular Biology* **426** 39–42
[13] Ptashne M and Gann A 2002 *Genes and Signals* (Cold Spring Harbor Laboratory Press)
[14] Ryerson S and Enciso G A 2014 *Journal of Mathematical Biology* **69** 977–999
[15] Buchler N E, Gerland U and Hwa T 2003 *Proceedings of the National Academy of Sciences* **100** 5136–5141
[16] Mazza C and Benaïm M 2014 *Stochastic Dynamics for Systems Biology* (CRC Press)
[17] Scatchard G 1949 *Annals of the New York Academy of Sciences* **51** 660–672
[18] Koshland D, Nemethy G and Filmer D 1966 *Biochemistry* **5** 365–385
[19] McGhee J D and von Hippel P H 1974 *Journal of Molecular Biology* **86** 469–489
[20] Ellis R S 1985 *Entropy, Large Deviations and Statistical Mechanics* (Springer)
[21] Di Biasio A, Agliari E, Barra A and Burioni R 2012 *Theoretical Chemistry Accounts* **131** 1104
[22] Lando D Y and Teif V B 2000 *Journal of Biomolecular Structure and Dynamics* **17** 903–911
[23] Vtyurina N V, Dulin D, Docter M W, Meyer A S, Dekker N H and Abbondanzieri E A 2016 *Proceedings of the National Academy of Sciences* **113** 4982–4987
[24] Teif V B and Rippe K 2010 *Journal of Physics: Condensed Matter* **22** 414105

[25] Duke T, Le Novère N and Bray D 2001 *J. Mol. Biol.* **308** 541–553
[26] Bray D and Duke T 2004 *Annu. Rev. Biophys. Biomol. Struct.* **33** 53–73
[27] Ackers G K, Johnson A D and Shea M A 1982 *Proceedings of the National Academy of Sciences* **79** 1129–1133
[28] Senear D A and Ackers G K 1990 *Biochemistry* **29** 6568–6577
[29] E S, Fonduge-Mittendorf Y, Chen L, Thåström A, Fiely Y, Moore I K, Wang J Z and Widom J 2006 *Nature* **442** 772–778
[30] Raveh-Sdadka T, Levo M and Segal E 2009 *Genome Research* **19** 1480–1496
[31] Teif V B and Rippe K 2009 *Nucleic Acids Research* **37** 5641–5655
[32] Chevereau G, Palmeira L, Thermes C, Arneodo A and Vaillant C 2009 *Physical Review Letters* **103** 188103
[33] Beshnova D A, Cherstvy A G, Vainshtein Y and Teif V B 2014 *PLOS Computational Biology* **10** e1003698
[34] Mirny L A 2010 *Proceedings of the National Academy of Sciences* **107** 22534–22539
[35] Pettersson M and W S 1990 *Journal of Molecular Biology* **214** 373–380
[36] Miller J A and Widom J 2003 *Molecular and Cellular Biology* **23** 1623–1632
[37] Vashee S, Melcher K, Ding W V, Johnston S A and Kodakek T 1998 *Current Biology* **8** 452–458
[38] Adams C C and L W J 1995 *Molecular and Cellular Biology* **15** 1405–1421
[39] Monod J, Wyman J and Changeux J 1965 *Journal of Molecular Biology* **12** 88–118
[40] Agliari E, Altavilla M, Barra A, Dello Schiavo L and Katz E 2015 *Scientific Reports* **5** 9415
[41] Wang L, Nie Q and Enciso G 2010 *Biophysical journal* **99** L41–L43
[42] Hatakeyama T S and Kaneko K 2014 *PLoS Computational Biology* **10** e1003784
[43] Goldbetter A and Koshland D E 1981 *Proceedings of the National Academy of Sciences* **78** 6840–6844
[44] Goldbetter A and Koshland D E 1982 *Quarterly Reviews of Biophysics* **15** 555–591
[45] Di Cera E 1995 *Thermodynamic Theory of Site-Specific Binding Processes in Biological Macromolecules* (Cambridge University Press)
[46] Abeliovich H 2005 *Biophysical Journal* **89** 76–79
[47] Abeliovich H 2016 *Journal of Mathematical Biology* **76** 1399–1411
[48] Schellman J A 1990 *Biopolymers* **29** 215–224
[49] Dill K and Bromberg S 2003 *Molecular Driving Forces* (Garland Science)
[50] Ben-Or M and Linial N 1989 Collective coin flipping *Randomness and Computation* (JAI Press)
[51] Bourgain J, Kahn J, Kalai G, Katznelson Y and Linial N 1992 *Israel Journal of Mathematics* **77** 55–64
[52] Bezuindenhout C E, Grimmett G R and Kesten H 1993 *Communication in Mathematical Physics* **158** 1–16
[53] Graham B T and Grimmett G R 2006 *The Annals of Probability* **34** 1726–1745
[54] Friedgut E 2004 *Combinatorics, Probabability and Computing* **13** 17–29
[55] Kahn J, Kalai G and Linial N 1988 The influence of variables on boolean functions *Proceedings of the 29th Symposium on the Foundations of Computer Science* SFCS '88 pp 68–80
[56] Friedgut E and Kalai G 1996 *Proceedings of the American Mathematical Society* **124** 2993–3002
[57] Talagrand M 1994 *The Annals of Probability* **22** 1576–1587
[58] Ethier S N and Kurtz T G 1986 *Markov Processes: Characterization and Convergence* (Wiley)
[59] Chan T 1998 *The Journal of the Australian Mathematical Society. Series B. Applied Mathematics* **40** 238–256
[60] Markevich N, Hoek J and Khodolenko B 2004 *Journal of Cell Biology* **164** 353–359
[61] Bowman G R and Geissler P L 2012 *Proceedings of the National Academy of Sciences* **109** 11681–11686
[62] Bowman G R, Bolin E R, Hart K M, Magieire B C and Marquese S 2015 *Proceedings of the National Academy of Sciences* **112** 2734–2739
[63] DuBay K H, Bowman G R and Geissler P L 2015 *Accounts of Chemical Research* **48** 1098–1105